International Journal of Control, Automation and Systems 20(4) (2022) 1266-1274
http://dx.doi.org/10.1007/s12555-021-0116-y
ISSN:1598-6446 eISSN:2005-4092
http://www.springer.com/12555

A Novel Set-valued Observer Based State Estimation Algorithm for Nonlinear Systems

Shuai Zhang, Zi-Yun Wang*, Yan Wang, and Zhi-Cheng Ji

Abstract: This study considers the state estimation problem for nonlinear models with unknown but bounded noises. A zonotopic set-valued observer based state estimation algorithm is proposed, and the unknown noise term is wrapped in a zonotope during each recursive step. The second-order polynomial Stirling interpolation improves the linearization accuracy and reduces the calculation amount. The method that combines sequence updating and tightening strips reduces the accumulation of errors and improves the estimation accuracy. Finally, the simulations on the Van der Pol nonlinear model and spring-mass-damper nonlinear model can visually illustrate the feasible parameter set variation process and motion trail of the zonotope, which demonstrates the effectiveness and accuracy of the proposed algorithm.

Keywords: Filtering, nonlinear system, state estimation, unknown but bounded.

1. INTRODUCTION

In recent years, studies on sequence estimation methods have achieved remarkable results, facilitating the application of online modeling and model-based control methods [1–3]. Among the statistical-based system estimation methods, the Kalman filters are the most well-known [4,5]. This type of filter or state estimator uses the statistical prior knowledge of system measurement noise and process noise, such as white noise, to obtain the best estimated value by optimizing the minimum function of the expected estimated deviation value. Moreover, this algorithm includes only a prediction step and update step, which is convenient for online application. Therefore, this method is widely used, and its subsequent development of nonlinear system estimation methods, such as the extended Kalman filtering [6] and unscented Kalman filtering [7], has extended its application range. However, these estimation methods have a common feature, i.e., they require certain prior knowledge of the system's process noise and measurement noise, or they assume that the noise meets certain distribution conditions and only then can the model-based optimization problem reach the optimum. However, in practical systems and application environments, the statistical characteristics of noise are generally considerably complex and constantly change, rendering their accurate measurement and evaluation difficult. The statistical characteristics of noise are assumed to be inconsistent with the actual system, which in turn will cause deviations in the filter, and owing to the noise sensitivity of the Kalman filter, the estimated deviation will be amplified and the estimator will become unstable as well. Although several adaptive mechanisms have been incorporated into the Kalman filter [8], the shortcomings of the Kalman filter's dependence on statistical characteristics and strong sensitivity have led to its application limitations.

Although the statistical characteristics of noise in actual systems are generally difficult to predict, the noise can be assumed to be bounded. The set-membership filter is based on bounded noise assumptions and provides a feasible bound for the state of the system by calculating the feasible set [9]. In this manner, the estimation result ceases to be a value and becomes a feasible set of parameters. This feasible set describes all the possible values of the system ensuring that the true value must be included in the set. The feasible set of parameters can be represented by different standard geometries, such as ellipsoid [10,11], interval [12], orthotope [13], parallelotope [14], zonotope *et al.* [15–17]. Among these, the method using the ellipsoid as the feasible set of parameters is the most widely used because of its invariance under the affine transformation and the significance of the covariance of the envelope matrix to facilitate optimization.

Manuscript received February 10, 2021; revised April 16, 2021; accepted June 11, 2021. Recommended by Associate Editor Shun-ichi Azuma under the direction of Editor Hamid Reza Karimi. This work is supported in part by the the National Key Research and Development Program of China (2020YFB1710600), the Jiangsu Science and Technology Association Young Science and Technology Talents Lifting Project (TJ-2021-006) and the National Natural Science Foundation of China (61973138).

Shuai Zhang, Zi-Yun Wang, Yan Wang, and Zhi-Cheng Ji are with the Engineering Research Center of Internet of Things Technology and Applications (Ministry of Education), School of Internet of Things Engineering, Jiangnan University, Wuxi 214122, China (e-mails: zshuai_9508@163.com, wangzy0601@163.com, yanwang@jiangnan.edu.cn, zcji@jiangnan.edu.cn).
* Corresponding author.

By combining Kalman filter and set-membership filter, Scholte *et al.* proposed extended set-membership filter (ESMF) [18]. Different from the Kalman filter, ESMF adopts Taylor expansion to linearize nonlinear systems and uses linearization errors as virtual process noises. However, disadvantages such as poor numerical stability and difficult selection of filter parameters exist. Since then, using the set membership identification method to process the state estimation [19] and model predict control [20] of the nonlinear system have received wide attention. A factorization-based nonlinear adaptive extended set-membership filter (AESMF) has been proposed [21]. In this method, each envelope matrix in the algorithm is expressed and updated in the form of decomposition. Furthermore, the filter parameters can be adaptively selected. By combining the sequence update and selection update strategies of observations, the stability of the algorithm is strengthened and the selection update reduces the computational complexity of the algorithm [22]. As the above methods adopt the Taylor expansion method for the process of linearizing the nonlinear system, certain disadvantages arise. For example, for strongly nonlinear systems, ESMF can cause large linearization errors, making it difficult to stabilize the filter. Furthermore, Jacobian matrices and their power calculations are complex, error-prone, and the points of the function are differentiable, thereby increasing the difficulty in using ESMF. Simultaneously, the linearization error boundary determined by the interval analysis method is excessively conservative. In addition, the solution of complex differential equations obtained by minimizing the volume or trace of the ellipsoid in the measurement update obstructs the implementation of the algorithm. A method using interpolation linearization is proposed [23], and the measurement update is relaxed up to the intersection of the strips while improving the method of iteratively determining the intersection [24].

Differing from the previously proposed algorithms, this paper uses a zonotope as the parameter feasible set. A central difference zonotopic set-valued observer based state estimation algorithm is proposed. The main contributions of this paper are listed as follows: 1) The second-order polynomial Stirling interpolation formula is used to make the nonlinear error smaller. Reduce the complexity of the algorithm without determining Jacobian and Hessian matrices; 2) when solving the virtual process noise, it is not necessary to repeatedly use the box to wrap the ellipsoid and vice versa. The error range can be locked directly through the vertices of the zonotope and the conservativeness of the algorithm is thus reduced; 3) in the process of sequence updating, constraints are optimized to reduce the impact of error accumulation on the algorithm and improve estimation accuracy. And the dimensionality reduction of singular value decomposition (SVD) of zonotope reduces the computational complexity.

Briefly, the rest of this paper is organized as follows: Section 2 presents the system description. Section 3 presents a central differential zonotope set-membership filter for state estimation. Section 4 provides the simulations to illustrate the accuracy and effectiveness of the proposed algorithm. Section 5 gives the conclusions.

2. SYSTEM DESCRIPTION

Firstly, certain preliminary notations are introduced. An interval $[a,b]$ is the set $\{x : a \leqslant x \leqslant b\}$. $\mathbf{B} = [-1,1]$ represents the unitary interval, and a box of order l is denoted as $\mathbf{B}^l$ that is composed by l unitary intervals [25]. The notation $f^{(i)}$ is the derivative of order i, H^{T} represents the transpose of matrix H, and $H^{i,\mathrm{T}}$ represents the transpose of matrix H^i. $\|f(x)\|_1$ denotes the 1 norm of function $f(x)$, If function $f(x)$ is a vector $f(x) = [x_1,x_2,\cdots,x_n]$, 1 norm of $f(x)$ is $|x_1|+|x_2|+\cdots+|x_n|$. If function $f(x)$ is a matrix, 1 norm of $f(x)$ is $\max\limits_{1\leq j\leq n}\sum\limits_{i=1}^{n}|x_{ij}|$, where n is the number of columns and x_{ij} represents the element in the ith row and jth column.

Definition 1: The Minkowski sum of two zonotopes is defined as $\Psi_s = \{\boldsymbol{x} : \boldsymbol{x} = \boldsymbol{x}_1+\boldsymbol{x}_2, \boldsymbol{x}_1 \in \mathcal{Z}_1, \boldsymbol{x}_2 \in \mathcal{Z}_2\}$ and it can also be expressed as $\Psi_s = \mathcal{Z}_1 \oplus \mathcal{Z}_2$.

Definition 2: $\mathcal{Z} = p \oplus H\mathbf{B}^l = \{p+Hz : z \in \mathbf{B}^l\}$, simplified as $\mathcal{Z}(p,H)$, is defined as a zonotope of order l, where $p \in \mathbb{R}^n$ is the center of the zonotope and matrix $H \in \mathbb{R}^{n\times l}$.

Consider an uncertain nonlinear discrete-time system,

$$\begin{aligned} \boldsymbol{x}_{k+1} &= \boldsymbol{f}(\boldsymbol{x}_k)+\boldsymbol{w}_k, \\ \boldsymbol{y}_k &= \boldsymbol{q}(\boldsymbol{x}_k)+\boldsymbol{v}_k, \end{aligned} \tag{1}$$

where $\boldsymbol{x}_{k+1} \in \mathbb{R}^{n_w}$ is the state of the system and $\boldsymbol{y}_k \in \mathbb{R}$ is the measured output vector. The vector $\boldsymbol{w}_k \in \mathbb{R}^{n_w}$ represents the process noise and the vector $\boldsymbol{v}_k \in \mathbb{R}^{n_v}$ is the measurement noise. $\boldsymbol{f}(\cdot)$ and $\boldsymbol{q}(\cdot)$, assumed as second-order reachable functions in ESMF and its extension algorithms, are known as nonlinear functions. Assuming that $\boldsymbol{x}_0 \in \mathcal{Z}_0$, and process noise and measurement noise terms satisfy $\boldsymbol{w}_k \in \mathcal{Z}(0,\boldsymbol{r}_w)$ and $\boldsymbol{v}_k \in \mathcal{Z}(0,\boldsymbol{r}_v)$, respectively.

3. CENTRAL DIFFERENCE ZONOTOPIC SET-VALUED OBSERVER

During the iterative update process, errors will accumulate as the number of iterations increases, and in the sequence update, if only the last step of the zonotope is considered, the error will be amplified. Therefore, to avoid the decrease in estimation accuracy caused by the accumulation of errors, the intersection of the strip and zonotope should be tightened first, and all zonotopes in the previous step need to be considered when updating in the present step. Next we consider the support planes of the zonotope and propose a method for strip tightening in the observer.

3.1. Nonlinear model linearization

As Jacobian matrix and Hessian matrix of Taylor series causes computational complexity, polynomial interpolation can be used to approximate nonlinear functions in an interval. Furthermore, most interpolation formulas do not require differentiation, thus it is considerably easier to obtain approximate values. Moreover, the accuracy of the interpolation formula can be set higher than the Taylor series of the same order by setting an appropriate step size. After transformation [26], the Stirling interpolation formula for the function $\boldsymbol{f}(\boldsymbol{x})$ centered on the point $\boldsymbol{x}=\bar{\boldsymbol{x}}$ can be transformed into

$$\begin{aligned}\boldsymbol{f}(\boldsymbol{x}) \approx& \boldsymbol{f}(\bar{\boldsymbol{x}})+\boldsymbol{f}'(\bar{\boldsymbol{x}})(\boldsymbol{x}-\bar{\boldsymbol{x}})+\frac{\boldsymbol{f}''(\bar{\boldsymbol{x}})}{2!}(\boldsymbol{x}-\bar{\boldsymbol{x}})^2\\ &+\left(\frac{\boldsymbol{f}^{(3)}(\bar{\boldsymbol{x}})}{3!}h^2+\frac{\boldsymbol{f}^{(5)}(\bar{\boldsymbol{x}})}{5!}h^4+\cdots\right)(\boldsymbol{x}-\bar{\boldsymbol{x}})\\ &+\left(\frac{\boldsymbol{f}^{(4)}(\bar{\boldsymbol{x}})}{4!}h^2+\frac{\boldsymbol{f}^{(6)}(\bar{\boldsymbol{x}})}{6!}h^4+\cdots\right)(\boldsymbol{x}-\bar{\boldsymbol{x}})^2,\end{aligned} \tag{2}$$

where h denotes a selected interval length.

Assuming that only the second-order polynomial Stirling interpolation formula is considered and extended to the high-dimensional case, the Stirling interpolation formula at $\boldsymbol{x}=\bar{\boldsymbol{x}}$ of $\boldsymbol{f}(\boldsymbol{x})$ can be expressed as

$$\boldsymbol{f}(\boldsymbol{x})=\boldsymbol{f}(\bar{\boldsymbol{x}})+\tilde{D}_{\Delta x}\boldsymbol{f}+\frac{1}{2!}\tilde{D}^2_{\Delta x}\boldsymbol{f}+H.O.T., \tag{3}$$

where $H.O.T.$ is the higher-order co-item of the Stirling interpolation formula of $\boldsymbol{f}(\cdot)$; the difference operators can be expressed as follows:

$$\tilde{D}_{\Delta x}\boldsymbol{f}=\frac{1}{h}\left(\sum_{i=1}^{n}\Delta x_i\mu_i\delta_i\right)\boldsymbol{f}(\bar{\boldsymbol{x}}), \tag{4}$$

$$\begin{aligned}\tilde{D}^2_{\Delta x}\boldsymbol{f}=&\frac{1}{h^2}\left(\sum_{i=1}^{n}\Delta x_i^2\delta_i^2\right.\\ &\left.+\sum_{i=1}^{n}\sum_{q=1,q\neq i}^{n}\Delta x_i\Delta x_q(\mu_i\delta_i)(\mu_q\delta_q)\right)\boldsymbol{f}(\bar{\boldsymbol{x}}),\end{aligned} \tag{5}$$

where μ_i is the i-th average operator and δ_i is the i-th difference operator. And the parameters $\delta_i\boldsymbol{f}(\bar{\boldsymbol{x}}),\mu_i\boldsymbol{f}(\bar{\boldsymbol{x}})$ and the first-order polynomial Stirling interpolation formula can be found in [27]. For the convenience of calculation, the second-order Stirling interpolation formula is simplified as

$$\boldsymbol{f}(\boldsymbol{x})\approx\boldsymbol{f}(\bar{\boldsymbol{x}})+\boldsymbol{f}'_{DD}(\bar{x})(\boldsymbol{x}-\bar{\boldsymbol{x}})+\frac{\boldsymbol{f}''_{DD}(\bar{\boldsymbol{x}})}{2!}(\boldsymbol{x}-\bar{\boldsymbol{x}})^2, \tag{6}$$

where

$$\boldsymbol{f}'_{DD}(\bar{\boldsymbol{x}})=\frac{\boldsymbol{f}(\bar{\boldsymbol{x}}+h\boldsymbol{e}_i)-\boldsymbol{f}(\bar{\boldsymbol{x}}-h\boldsymbol{e}_i)}{2h},$$
$$\boldsymbol{f}''_{DD}(\bar{\boldsymbol{x}})=\frac{\boldsymbol{f}(\bar{\boldsymbol{x}}+h\boldsymbol{e}_i)+\boldsymbol{f}(\bar{\boldsymbol{x}}-h\boldsymbol{e}_i)-2\boldsymbol{f}(\bar{\boldsymbol{x}})}{h^2}.$$

Expanding $\boldsymbol{f}(\boldsymbol{x}_k)$ in (1) into the form of (6) at state $\hat{\boldsymbol{x}}_k$

$$\boldsymbol{f}(\boldsymbol{x}_k)\approx\boldsymbol{f}(\hat{\boldsymbol{x}}_k)+\boldsymbol{F}'_k(\boldsymbol{x}_k-\hat{\boldsymbol{x}}_k)+\boldsymbol{F}''_k(\boldsymbol{x}_k-\hat{\boldsymbol{x}}_k)^2, \tag{7}$$

where

$$\boldsymbol{F}'_k=\frac{1}{2h}\begin{bmatrix}(\boldsymbol{f}(\hat{\boldsymbol{x}}_k^{1+})-\boldsymbol{f}(\hat{\boldsymbol{x}}_k^{1-}))^{\mathrm{T}}\\ (\boldsymbol{f}(\hat{\boldsymbol{x}}_k^{2+})-\boldsymbol{f}(\hat{\boldsymbol{x}}_k^{2-}))^{\mathrm{T}}\\ \vdots\\ (\boldsymbol{f}(\hat{\boldsymbol{x}}_k^{n+})-\boldsymbol{f}(\hat{\boldsymbol{x}}_k^{n-}))^{\mathrm{T}}\end{bmatrix}^{\mathrm{T}},$$

$$\boldsymbol{F}''_k=\frac{1}{2h^2}\begin{bmatrix}(\boldsymbol{f}(\hat{\boldsymbol{x}}_k^{1+})+\boldsymbol{f}(\hat{\boldsymbol{x}}_k^{1-})-2\boldsymbol{f}(\hat{\boldsymbol{x}}_k^{1}))^{\mathrm{T}}\\ (\boldsymbol{f}(\hat{\boldsymbol{x}}_k^{2+})+\boldsymbol{f}(\hat{\boldsymbol{x}}_k^{2-})-2\boldsymbol{f}(\hat{\boldsymbol{x}}_k^{2}))^{\mathrm{T}}\\ \vdots\\ (\boldsymbol{f}(\hat{\boldsymbol{x}}_k^{n+})+\boldsymbol{f}(\hat{\boldsymbol{x}}_k^{n-})-2\boldsymbol{f}(\hat{\boldsymbol{x}}_k^{n}))^{\mathrm{T}}\end{bmatrix}^{\mathrm{T}},$$

and $\hat{\boldsymbol{x}}_k^{i+}=\hat{\boldsymbol{x}}_k+h\boldsymbol{e}_i,\hat{\boldsymbol{x}}_k^{i-}=\hat{\boldsymbol{x}}_k-h\boldsymbol{e}_i,\hat{\boldsymbol{x}}_k^{i}=\hat{\boldsymbol{x}}_k$.

3.2. Bounded linearization error

Assuming that $\boldsymbol{f}(\boldsymbol{x})$ is the difference of convex function on a convex set S, then there are two convex functions $g_1(\boldsymbol{x})$ and $g_2(\boldsymbol{x})$ such that $\boldsymbol{f}(\boldsymbol{x})=g_1(\boldsymbol{x})-g_2(\boldsymbol{x})$. The convex hypothesis of $\boldsymbol{f}(\boldsymbol{x})$ is easy to satisfy, because $\boldsymbol{f}(\boldsymbol{x})$ is a second-order continuous differentiable function, and each continuous function can be approximated by the function with arbitrary precision [24].

Assuming that $\frac{\partial^2\boldsymbol{f}(\boldsymbol{x})}{\partial\boldsymbol{x}^2}\geqslant-2\alpha I,\alpha\geqslant0$ and selecting $g_1(\boldsymbol{x})=\boldsymbol{f}(\boldsymbol{x})+\alpha\boldsymbol{x}^{\mathrm{T}}\boldsymbol{x}$, $g_2(\boldsymbol{x})=\alpha\boldsymbol{x}^{\mathrm{T}}\boldsymbol{x}$. The Stirling interpolation formula for the functions g_1 and g_2 at the current state point $\boldsymbol{x}_k$ can be expressed as

$$g_1(\boldsymbol{x}_k)\geqslant g_1(\hat{\boldsymbol{x}}_k)+G'_{1,k}(\boldsymbol{x}_k-\hat{\boldsymbol{x}}_k)+G''_{1,k}(\boldsymbol{x}_k-\hat{\boldsymbol{x}}_k)^2, \tag{8}$$
$$g_2(\boldsymbol{x}_k)\geqslant g_2(\hat{\boldsymbol{x}}_k)+G'_{2,k}(\boldsymbol{x}_k-\hat{\boldsymbol{x}}_k)+G''_{2,k}(\boldsymbol{x}_k-\hat{\boldsymbol{x}}_k)^2. \tag{9}$$

Define

$$\boldsymbol{f}_L(\boldsymbol{x}):=\boldsymbol{f}(\bar{\boldsymbol{x}})+\boldsymbol{f}'_{DD}(\bar{x})(\boldsymbol{x}-\bar{\boldsymbol{x}})+\frac{\boldsymbol{f}''_{DD}(\bar{\boldsymbol{x}})}{2!}(\boldsymbol{x}-\bar{\boldsymbol{x}})^2, \tag{10}$$

$$\bar{g}_1(\boldsymbol{x}_k):=g_1(\hat{\boldsymbol{x}}_k)+G'_{1,k}(\boldsymbol{x}_k-\hat{\boldsymbol{x}}_k)+G''_{1,k}(\boldsymbol{x}_k-\hat{\boldsymbol{x}}_k)^2, \tag{11}$$

$$\bar{g}_2(\boldsymbol{x}_k):=g_2(\hat{\boldsymbol{x}}_k)+G'_{2,k}(\boldsymbol{x}_k-\hat{\boldsymbol{x}}_k)+G''_{2,k}(\boldsymbol{x}_k-\hat{\boldsymbol{x}}_k)^2. \tag{12}$$

The linearization error $e(k)=\boldsymbol{f}(\boldsymbol{x}_k)-\boldsymbol{f}_L(\boldsymbol{x}_k)=g_1(\boldsymbol{x}_k)-g_2(\boldsymbol{x}_k)-\boldsymbol{f}_L(\boldsymbol{x}_k)$, and $\bar{g}_1-g_2-\boldsymbol{f}_L$ is a concave function while $g_1-\bar{g}_2-\boldsymbol{f}_L$ is a convex function. Thus, the range of $e(k)$ is

$$\begin{aligned}&\Big[\min_{\boldsymbol{x}_k\in V_S}\{\bar{g}_1(\boldsymbol{x}_k)-g_2(\boldsymbol{x}_k)-\boldsymbol{f}_L(\boldsymbol{x}_k)\},\\ &\max_{\boldsymbol{x}_k\in V_S}\{g_1(\boldsymbol{x}_k)-\bar{g}_2(\boldsymbol{x}_k)-\boldsymbol{f}_L(\boldsymbol{x}_k)\}\Big],\end{aligned} \tag{13}$$

where V_S involves the vertices of the feasible parameter set (FPS), and then the linearization error is wrapped with the minimum volume zonotope $\mathcal{Z}(\boldsymbol{a}_e,\boldsymbol{r}_e)$, where

$$\boldsymbol{a}_e = (\boldsymbol{e}_{k,\max}+\boldsymbol{e}_{k,\min})/2,$$
$$\boldsymbol{r}_e = (\boldsymbol{e}_{k,\max}-\boldsymbol{e}_{k,\min})/2.$$

Then the total process noise is the Minkowski sum of the linearization noise and process noise:

$$\mathcal{Z}(\boldsymbol{a}_e,\boldsymbol{r}_e)\oplus\mathcal{Z}(\boldsymbol{0},\boldsymbol{r}_w)=\mathcal{Z}(\boldsymbol{a}_e,[\boldsymbol{r}_e+\boldsymbol{r}_w]). \tag{14}$$

3.3. Time update

Assuming that the feasible parameter set at step k is $\mathcal{Z}_k = p_k \oplus H_k\mathbf{B}^l$. According to the zonotope formula, the vertices of the FPS can be obtained, and the predicted zonotope $\tilde{\mathcal{Z}}_k = f(p_k)\oplus\tilde{H}_k\mathbf{B}^l$ can be obtained by predicting the vertices and center point of the zonotope, respectively. Then the time updated zonotope is the Minkowski sum of the total process noise and predicted zonotope

$$\begin{aligned}\mathcal{Z}_{k+1,k} &= p_{k+1,k}\oplus H_{k+1,k}\mathbf{B}^{l+r_{ew}}\\ &= f(p_k)\oplus[\tilde{H}_k,\boldsymbol{r}_e+\boldsymbol{r}_w]\mathbf{B}^{l+r_{ew}},\end{aligned} \tag{15}$$

where r_{ew} is the number of columns in the matrix $\boldsymbol{r}_e+\boldsymbol{r}_w$.

3.4. Observation update

The function $\boldsymbol{q}(\cdot)$ of (1) can be approximated by the first-order polynomial Stirling interpolation formula at a predicted state $\hat{\boldsymbol{x}}_{k+1,k}$ as

$$\boldsymbol{q}(\boldsymbol{x}_{k+1,k})=\boldsymbol{q}(\hat{\boldsymbol{x}}_{k+1,k})+\boldsymbol{Q}'_{k+1}(\boldsymbol{x}_{k+1,k}-\hat{\boldsymbol{x}}_{k+1,k})+\boldsymbol{o}_k, \tag{16}$$

where

$$\boldsymbol{Q}'_{k+1}=\frac{1}{2h}\begin{bmatrix}(\boldsymbol{q}(\hat{\boldsymbol{x}}^{1+}_{k+1,k})-\boldsymbol{q}(\hat{\boldsymbol{x}}^{1-}_{k+1,k}))^{\mathrm{T}}\\(\boldsymbol{q}(\hat{\boldsymbol{x}}^{2+}_{k+1,k})-\boldsymbol{q}(\hat{\boldsymbol{x}}^{2-}_{k+1,k}))^{\mathrm{T}}\\\vdots\\(\boldsymbol{q}(\hat{\boldsymbol{x}}^{n+}_{k+1,k})-\boldsymbol{q}(\hat{\boldsymbol{x}}^{n-}_{k+1,k}))^{\mathrm{T}}\end{bmatrix}^{\mathrm{T}}, \tag{17}$$

and $\hat{\boldsymbol{x}}^{i+}_{k+1,k}=\hat{\boldsymbol{x}}_{k+1,k}+h\boldsymbol{e}_i, \hat{\boldsymbol{x}}^{i-}_{k+1,k}=\hat{\boldsymbol{x}}_{k+1,k}-h\boldsymbol{e}_i, \hat{\boldsymbol{x}}^{i}_{k+1,k}=\hat{\boldsymbol{x}}_{k+1,k}$ and $\boldsymbol{o}_k$ is the linearization error.

Similarly, according to the processing described in the first few sections, the total measurement noise can be obtained as

$$\mathcal{Z}(\boldsymbol{a}_o,\boldsymbol{r}_o)\oplus\mathcal{Z}(\boldsymbol{0},\boldsymbol{r}_v)=\mathcal{Z}(\boldsymbol{a}_o,[\boldsymbol{r}_o+\boldsymbol{r}_v]), \tag{18}$$

where $\mathcal{Z}(\boldsymbol{a}_o,\boldsymbol{r}_o)$ is the linearization error of the measurement equation, and $\mathcal{Z}(\boldsymbol{0},\boldsymbol{r}_v)$ is the input error of the measurement equation.

The observation set can be expressed as

$$S_{k+1}=\Big\{\boldsymbol{x}:|\boldsymbol{y}_{k+1}-\boldsymbol{q}(\hat{\boldsymbol{x}}_{k+1,k})+\boldsymbol{Q}'_{k+1}(\hat{\boldsymbol{x}}_{k+1,k}-\boldsymbol{x})|\leqslant\boldsymbol{r}_o+\boldsymbol{r}_v\Big\}. \tag{19}$$

Equation (19) can be viewed as the intersection of m independent strips

$$\bigcap_{i=1}^{m}S_{k+1,i}=\bigcap_{i=1}^{m}\{\boldsymbol{x}:|y^a_{k+1,i}-\boldsymbol{Q}'_{k+1,i}\boldsymbol{x}|\leqslant r^a_i\}, \tag{20}$$

where $y^a_{k+1,i}$ and r^a_i are the i-th components of $\boldsymbol{y}_{k+1}-\boldsymbol{q}(\hat{\boldsymbol{x}}_{k+1,k})+\boldsymbol{Q}'_{k+1}\hat{\boldsymbol{x}}_{k+1,k}$ and $\boldsymbol{r}_o+\boldsymbol{r}_v$, respectively.

Thus, the feasible set of parameters is derived as

$$\mathcal{Z}_{k+1}=\mathcal{Z}_{k+1,k}\bigcap(\bigcap_{i=1}^{m}S_{k+1,i}). \tag{21}$$

As $\bigcap_{i=1}^{m}S_{k+1,i}$ is a polyhedron, it is usually difficult to solve the intersection of a polyhedron and zonotope. Equation (21) is decomposed into the intersection of a zonotope with m strips. Initialize iteration zonotope as in (15), where $p^0=p_{k+1,k}$, $H^0=H_{k+1,k}$.

Assuming that the i-th strip is $\{\boldsymbol{x}:|c^{\mathrm{T}}\boldsymbol{x}-d|\leqslant\sigma\}$. Then the iterative formulas are

$$v(j)=\begin{cases}p^{i-1}+\left(\dfrac{d-c^{\mathrm{T}}p}{c^{\mathrm{T}}H^{i-1}_j}\right)H^{i-1}_j,\\ \qquad\qquad \text{if } 1\leqslant j\leqslant r \text{ and } \mathrm{c}^{\mathrm{T}}H^{i-1}_j\neq 0,\\ p^{i-1}, \quad \text{otherwise,}\end{cases} \tag{22}$$

$$T(j)=\begin{cases}\left[T^j_1T^j_2\dots T^j_r\right], & \text{if } 1\leqslant j\leqslant r \text{ and } c^{\mathrm{T}}H^{i-1}_j\neq 0,\\ H^{i-1}, & \text{otherwise,}\end{cases} \tag{23}$$

$$T^j_l=\begin{cases}H^{i-1}_l-\left(\dfrac{c^{\mathrm{T}}H^{i-1}_l}{c^{\mathrm{T}}H^{i-1}_j}\right)H^{i-1}_j, & \text{if } l\neq j,\\ \left(\dfrac{\sigma}{c^{\mathrm{T}}H^{i-1}_j}\right)H^{i-1}_j, & \text{if } l=j,\end{cases} \tag{24}$$

where r is the number of columns in the matrix H^{i-1} and

$$\begin{aligned}j^* &= \arg\min_{0\leqslant j\leqslant r}2^{n_w}\sqrt{\det(T(j)T(j)^{\mathrm{T}})}\\ &= \arg\min_{0\leqslant j\leqslant r}\det\left(T(j)T(j)^{\mathrm{T}}\right).\end{aligned} \tag{25}$$

Then $p^i=v(j^*), H^i=T(j^*)$ and $\mathcal{Z}_{k+1}=p^m\oplus H^m\mathbf{B}^{l+r_{ew}}$.

The specific process of central difference zonotopic set-valued observer based state estimation algorithm (CDZSVO) is given in Algorithm 1.

4. NUMERICAL EXAMPLES

Example 1: The following Van der Pol nonlinear discrete-time system is studied [28].

$$\begin{bmatrix}x_{1,k+1}\\x_{2,k+1}\end{bmatrix}=\begin{bmatrix}x_{1,k}+hx_{2,k}\\x_{2,k}+h\delta_{2,k}\end{bmatrix}+\boldsymbol{w}_k,$$

Algorithm 1: Framework of the CDZSVO algorithm

Input: The initial zonotope $\mathscr{Z}_0 = p_0 \oplus H_0\mathbf{B}^l$ and system output y_k.
Output: The parameter estimate $\boldsymbol{x}_{k+1}$ and final zonotope $\mathscr{Z}_k = p_k \oplus H_k\mathbf{B}^l$

$k \leftarrow 0$, $L \leftarrow$ Constant;
Initialization: Selected initial length h, $\mathscr{Z}_0 = p_0 \oplus H_0\mathbf{B}^l$, initial state $\boldsymbol{x}_0 = p_0$;
for $k = 1 : L$ **do**
  Linearize the function $\boldsymbol{f}(\cdot)$ at the state point $\boldsymbol{x}_k$;
  Set the DC functions $g_1(\boldsymbol{x})$, $g_2(\boldsymbol{x})$, and linearize to obtain $\bar{g}_1(\boldsymbol{x})$, $\bar{g}_2(\boldsymbol{x})$;
  According to (13), the bounded linearization error is obtained;
  According to (14), calculate the total process noise;
  Update time and obtain $\mathscr{Z}_{k+1,k} = p_{k+1,k} \oplus H_{k+1,k}\mathbf{B}^{l+r_{ew}}$;
  Obtain the linearization error of the function $\boldsymbol{q}(\boldsymbol{x})$ according to the same method;
  Observation update: Initialize iteration zonotope $p^0 = p_{k+1,k}$, $H^0 = H_{k+1,k}$;
  for $j = 1 : m$ **do**
    Obtain the i-th strip from Eq.(20) and calculate the support planes of the zonotope: $q_{u,0} = c^{\mathrm{T}}p^0 + \|H^{0,\mathrm{T}}c\|_1, q_{l,0} = c^{\mathrm{T}}p^0 - \|H^{0,\mathrm{T}}c\|_1$;
    if $y+\sigma > q_{u,0} > y-\sigma > q_{l,0}$ **then**
      $y = \frac{q_{u,0}+y-\sigma}{2}, \sigma = \frac{q_{u,0}-y+\sigma}{2}$;
    else if $y+\sigma > q_{u,0} > q_{l,0} > y-\sigma$ **then**
      $y = \frac{q_{u,0}+q_{l,0}}{2}, \sigma = \frac{q_{u,0}-q_{l,0}}{2}$;
      else if $q_{u,0} > y+\sigma > q_{l,0} > y-\sigma$ **then**
        $y = \frac{y+\sigma+q_{l,0}}{2}, \sigma = \frac{y+\sigma-q_{l,0}}{2}$;
      end
    end
    end
    if $j \geqslant 1$ **then**
      for $i = 1 : j$ **do**
        Calculating the support planes of the zonotope: $q_{u,i} = c^{\mathrm{T}}p^i + \|H^{i,\mathrm{T}}c\|_1, q_{l,i} = c^{\mathrm{T}}p^i - \|H^{i,\mathrm{T}}c\|_1$;
        if $y+\sigma > q_{u,i} > y-\sigma > q_{l,i}$ **then**
          $y = \frac{q_{u,i}+y-\sigma}{2}, \sigma = \frac{q_{u,i}-y+\sigma}{2}$;
        else if $y+\sigma > q_{u,i} > q_{l,i} > y-\sigma$ **then**
          $y = \frac{q_{u,i}+q_{l,i}}{2}, \sigma = \frac{q_{u,i}-q_{l,i}}{2}$;
          else if $q_{u,i} > y+\sigma > q_{l,i} > y-\sigma$ **then**
            $y = \frac{y+\sigma+q_{l,i}}{2}, \sigma = \frac{y+\sigma-q_{l,i}}{2}$;
          end
        end
        end
      end
    end
    According to (22), (23), (24), and (25), obtain the i-th iteration zonotope $p^i = v(j^*), H^i = T(j^*)$;
  end
end
Using SVD to reduce the dimension of the zonotope;
return k-th zonotope $\mathscr{Z}_k = p_k \oplus H_k\mathbf{B}^l$ and the state $\boldsymbol{x}_{k+1}$;

$$\boldsymbol{y}_k = \begin{bmatrix} 0 & 1 \\ 1 & 0 \end{bmatrix} \begin{bmatrix} x_{1,k} \\ x_{2,k} \end{bmatrix} + \boldsymbol{v}_k, \tag{26}$$

where $\delta_{2,k} = -9x_{1,k} + \mu\left(1 - x_{1,k}^2\right)x_{2,k}$. The initial conditions are $h = 0.02$, $\mu = 2$, $\boldsymbol{x}_0 = (1,2)^{\mathrm{T}}$, $p_0 = (1,2)^{\mathrm{T}}$, and $H_0 = diag(0.1, 0.1)$. The process and measurement disturbances are uniformly distributed and $|w_{k,i}| \leqslant 0.01$, $|v_{k,i}| \leqslant 0.001$.

In comparison to the central difference set-membership filtering (CDSMF) algorithm that is described in [23], the simulation results are shown in the Figs. 1-3.

- Fig. 1 shows the state trajectories and changes in the FPS of the two algorithms. As can be seen from the Fig. 1, both algorithms track the true trajectory well.

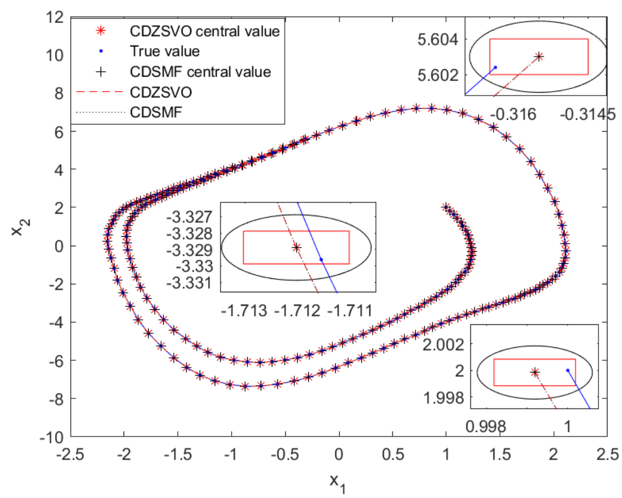

Fig. 1. Comparison of state trajectories and feasible parameter sets between CDZSVO and CDSMF algorithms.

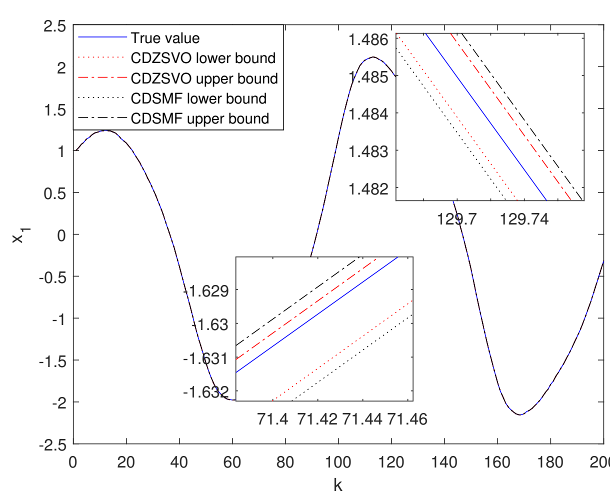

Fig. 2. Comparison of guaranteed bounds and centers of state x_1 between CDZSVO and CDSMF algorithms.

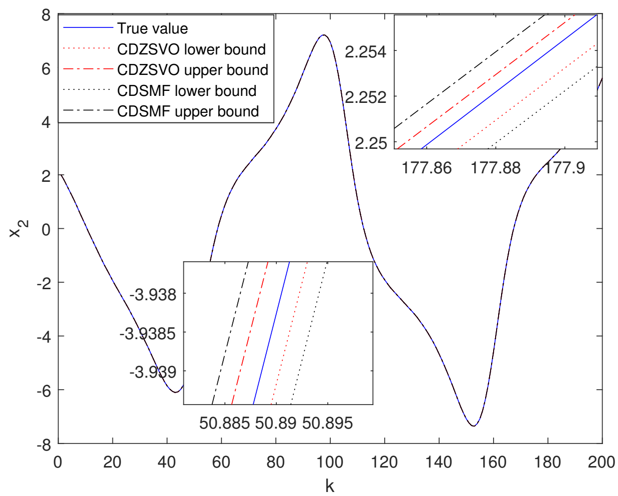

Fig. 3. Comparison of guaranteed bounds and centers of state x_2 between CDZSVO and CDSMF algorithms.

It should be noted that the state trajectory is only a mathematical probability, not a real motion trajectory. In the upper right corner, lower right corner, and middle position of Fig. 1, an enlarged graph of the FPS at time $k = 200$, time $k = 1$, and random time is given. The FPS of CDZSVO is always smaller than the one of CDSMF, which illustrates that CDZSVO is less conservative than CDSMF.

- In Figs. 2 and 3, the state boundary of both algorithms can contain true values. However, compared with CDSMF, the CDZSVO proposed in this paper can obtain tighter boundaries that can be also verified from Fig. 1. Again, the conservative improvement of this algorithm is demonstrated, showing the superiority of this algorithm.

Example 2: A spring-mass-damper nonlinear system estimation example in [18,22,23] is also given to illustrate the effectiveness of the proposed algorithm and its diagram is shown as Fig. 4. The discrete-time system of the Duffing equation can be expressed as

$$\begin{bmatrix} x_{1,k+1} \\ x_{2,k+1} \end{bmatrix} = \begin{bmatrix} x_{1,k-1} + \Delta T x_{2,k-1} \\ x_{2,k-1} + \Delta T \delta_{2,k-1} \end{bmatrix} + \boldsymbol{w}_k,$$
$$\boldsymbol{y}_k = \begin{bmatrix} 1 & 0 \end{bmatrix} \begin{bmatrix} x_{1,k} \\ x_{2,k} \end{bmatrix} + \boldsymbol{v}_k, \tag{27}$$

where $\delta_{2,k-1} = -k_0 x_{1,k-1}(1 + k_d x_{1,k-1}^2) - c x_{2,k-1}$. The process and measurement disturbances are uniformly distributed. For the simulations to follow the system parameters, the initial setting parameters are shown in Table 1 [18]. In comparison to ESMF that is described in [18] and CDSMF that is described in [23], the results are shown in the Figs. 5-10.

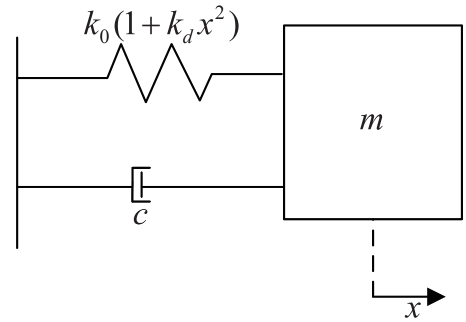

Fig. 4. The spring-mass-damper system.

Table 1. Parameters of the spring-mass-damper nonlinear system.

Parameter	Value
ΔT	0.1
k_d	3
k_0	1.5
c	1.24
$\boldsymbol{x}_0$	$(1,2)^{\mathrm{T}}$
w_k	0.002
v_k	10.001
p_0	$(1,2)^{\mathrm{T}}$
H_0	$diag(0.06, 0.06)$

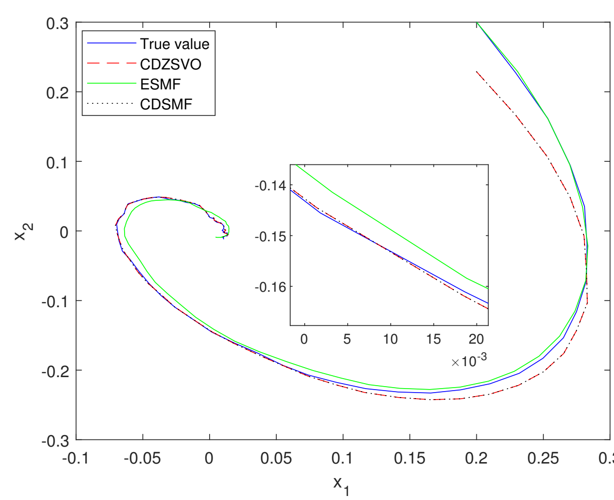

Fig. 5. Comparison of state trajectories between CDZSVO, CDSMF and ESMF algorithms.

- As can be seen from Fig. 5, all three algorithms can track the true value trajectory very well. Although CDZSVO and CDSMF did not work well at the beginning of the algorithm, they still converged to the true value at the end. Fig. 6 shows the changes of the feasible parameter set of CDZSVO and CDSMF. The feasible parameter sets of the two algorithms always wrap the true value, and the feasible parameter set of CDZSVO is smaller than CDSMF.

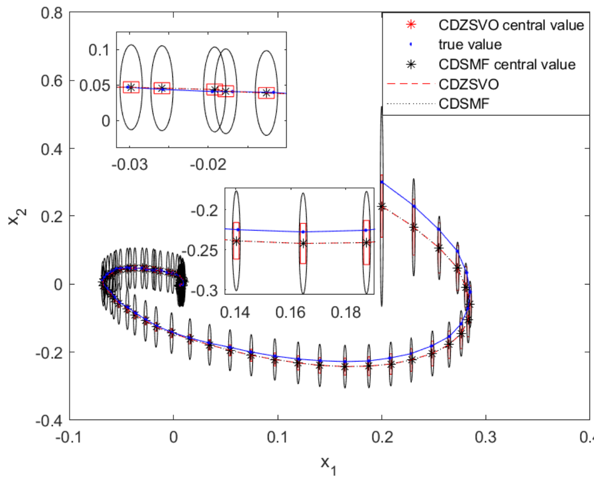

Fig. 6. Comparison of feasible sets between CDZSVO and CDSMF algorithms.

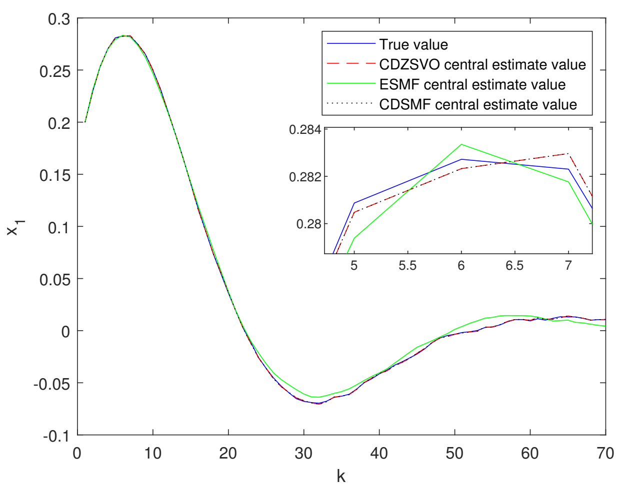

Fig. 7. Comparison of state estimation of x_1 between CDZSVO, CDSMF and ESMF algorithms.

- Figs. 7 and 8 show the variation curves of the center estimates and true values of the three algorithms. Although the CDZSVO and CDSMF center estimates are the same, the performance of the three algorithms is similar irrespective of state x_1 or x_2.
- The guaranteed bounds for states x_1 and x_2 are shown in Figs. 9 and 10. It can be seen that the state bounds of the three algorithms can contain true value; however, CDZSVO is more compact than CDSMF and ESMF, indicating that the algorithm proposed in this paper has made a large improvement on conservativeness.

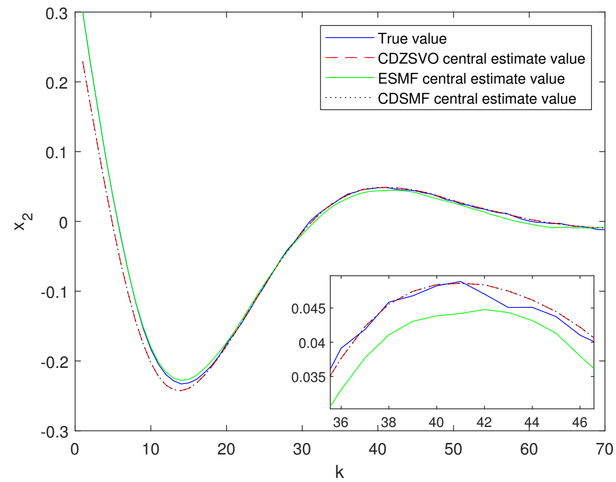

Fig. 8. Comparison of state estimation of x_2 between CDZSVO, CDSMF and ESMF algorithms.

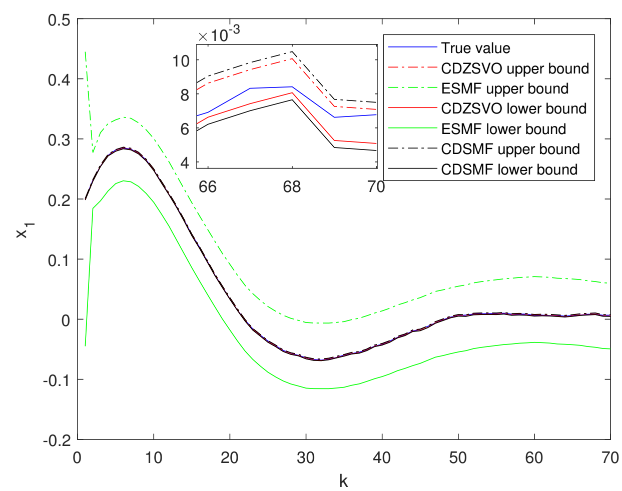

Fig. 9. Comparison of guaranteed bounds of state x_1 between CDZSVO, CDSMF and ESMF algorithms.

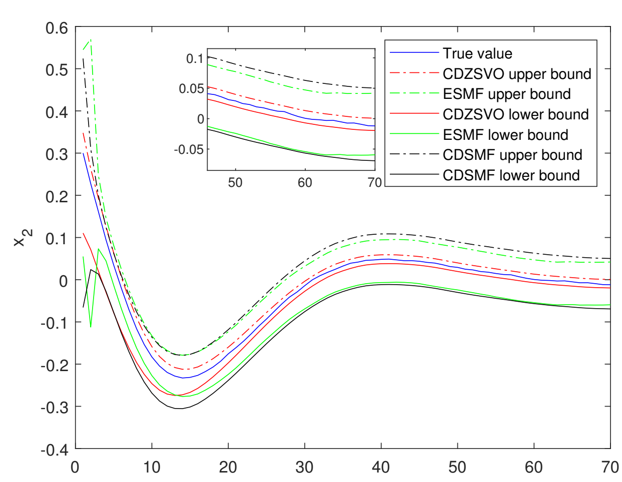

Fig. 10. Comparison of guaranteed bounds of state x_2 between CDZSVO, CDSMF and ESMF algorithms.

5. CONCLUSIONS

A new set-member filtering method is proposed to solve the state estimation problem of unknown but bounded noise nonlinear systems. First, the nonlinear system is linearized by the second-order polynomial Stirling interpolation to further reduce linearization error. Simultaneously, the uncertainty caused by the linearization error is considered, and its boundary is determined by the difference of convex function. Next, the observation set is decomposed into the intersection of multiple bands and a serialized update method is used to determine the FPS. To avoid errors caused by iteration, a method of tight strips and zonotope is proposed. To avoid greater computational complexity, using SVD technology to reduce the dimensionality of zonotopes. Finally, the performance advantages of the proposed algorithm in point estimation and boundary estimation are verified by simulation.

The proposed algorithms can also be further applied to combine with the robust control algorithms and to solve the state estimation of switched systems [29–31] and other nonlinear models [32,33], and future research work also includes exploring high-performance delimitation methods, and experimental verification of the filtering algorithm [34,35].

REFERENCES

[1] Y. Gao, Y. F. Wu, and X. Wang, "Characteristic model-based adaptive control with genetic algorithm estimators for four-PMSM synchronization system," *International Journal of Control, Automation, and Systems*, vol. 18, no. 6, pp. 1605-1616, June 2020.

[2] J. Voros, "Iterative identification of nonlinear dynamic systems with output backlash using three-block cascade models," *Nonlinear Dynamics*, vol. 79, no. 3, pp. 2187–2195, February 2015.

[3] M. H. Li, S. F. Hu, and J. W. Xia, "Dissolved oxygen model predictive control for activated sludge process model based on the fuzzy C-means cluster algorithm," *International Journal of Control, Automation, and Systems*, vol. 18, no. 9, pp. 2435-2444, September 2020.

[4] T. Shao, Z. S. Duan, and Q. B. Ge, "Recursive performance ranking of Kalman filter with mismatched noise covariances," *IET Control Theory & Applications*, vol. 13, no. 4, pp. 459-466, March 2019.

[5] F. Deng, H. L. Yang, and L. J. Wang, "Adaptive unscented Kalman filter based estimation and filtering for dynamic positioning with model uncertainties," *International Journal of Control, Automation, and Systems*, vol. 17, no. 3, pp. 667-678, March 2019.

[6] K. Xiong, H. Zhang, and L. Liu, "Adaptive robust extended Kalman filter for nonlinear stochastic systems," *IET Control Theory & Applications*, vol. 2, no. 3, pp. 239-250, March 2008.

[7] M. Tang, Z. Chen, and F. L. Yin, "Robot tracking in SLAM with masreliez-martin unscented Kalman filter," *International Journal of Control, Automation, and Systems*, vol. 18, no. 9, pp. 2315-2325, September 2020.

[8] L. Q. Zhao, J. L. Wang, and T. Yu, "Design of adaptive robust square-root cubature Kalman filter with noise statistic estimator," *Applied Mathematics and Computation*, vol. 256, pp. 352-367, April 2015.

[9] D. Ding, Z. Wang, and Q. Han, "A set-membership approach to event-triggered filtering for general nonlinear systems over sensor networks," *IEEE Transactions on Automatic Control*, vol. 65, no. 4, pp. 1792-1799, April 2020.

[10] Z. Y. Wang, Y. Wang, and Z. C. Ji, "A novel two-stage estimation algorithm for nonlinear Hammerstein-Wiener systems from noisy input and output data," *Journal of the Franklin Institute*, vol. 354, pp. 1937-1944, March 2017.

[11] Z. Y. Wang, Z. Tang, and J. H. Park, "A novel two-stage ellipsoid filtering-based system modeling algorithm for a Hammerstein nonlinear model with an unknown noise term," *Nonlinear Dynamics*, vol. 98, no. 4, pp. 2919–2925, December 2019.

[12] T. Raissi, N. Ramdani, and Y. Candus, "Set membership parameter estimation in the frequency domain based on complex intervals," *International Journal of Control, Automation, and Systems*, vol. 7, no. 5, pp. 824-834, October 2009.

[13] M. Casini, A. Garulli, and A. Vicino, "A linear programming approach to online set membership parameter estimation for linear regression models," *International Journal of Adaptive Control and Signal Processing*, vol. 31, no. 3, pp. 360-378, March 2017.

[14] U. Sharma and S. Thangavel, "Effective recursive parallelotopic bounding for robust output-feedback control," *IFAC Papers Online*, vol. 50, no. 15, pp. 1032-1037, 2018.

[15] J. M. Bravo, T. Alamo, and E. F. Camacho, "Bounded error identification of systems with time-varying parameters," *IEEE Transactions on Automatic Control*, vol. 55, no. 7, pp. 1144-1150, July 2006.

[16] J. Blesa, V. Puig, and J. Saludes, "Identification for passive robust fault detection using zonotope-based set-membership approaches," *International Journal of Adaptive Control and Signal Processing*, vol. 25, pp. 788-812, September 2011.

[17] W. Chai, X. F. Sun, and J. F. Qiao, "Set membership state estimation with improved zonotopic description of feasible solution set," *International Journal of Robust and Nonlinear Control*, vol. 23, pp. 1642-1654, September 2013.

[18] E. Scholte and M. E. Campbell, "A nonlinear set-membership filter for on-line applications," *International Journal of Robust and Nonlinear Control*, vol. 13, no. 15, pp. 1337-1358, December 2003.

[19] M. Milanese and C. Novara, "Set Membership identification of nonlinear systems,"*Automatica*, vol. 40, no. 6, pp. 957-975, June 2004.

[20] M. Canale, L. Fagiano, and M. C. Signorile, "Nonlinear model predictive control from data: A set membership approach,"*International Journal of Robust and Nonlinear Control*, vol. 24, no. 1, pp. 123-139, January 2014.

[21] B. Zhao, J. D. Han, and G. J. Liu, "A UD factorization-based nonlinear adaptive set membership filter for ellipsoidal estimation," *International Journal of Robust and Nonlinear Control*, vol. 18, no. 16, pp. 1513-1531, November 2008.

[22] B. Zhao, K. Qian, and X. D. Ma, "A new nonlinear set membership filter based on guaranteed bounding ellipsoid algorithm," *Acta Automatica Sinica*, vol. 39, no. 2, pp. 150-158, 2008.

[23] Q. Shen, J. Y. Liu, and Q. Zhao, "Central difference set-membership filter for nonlinear system," *Control Theory and Applications*, vol. 36, no. 8, pp. 1239-1249, 2019.

[24] T. Alamo, J. M. Bravo, and M. J. Redondo, "A set-membership state estimation algorithm based on DC programming," *Automatica*, vol. 44, no. 1, pp. 216-224, January 2008.

[25] T. Alamo, J. M, Bravo, and E. F. Camacho, "Guaranteed state estimation by zonotopes," *Automatica*, vol. 41, no. 6, pp. 1035-1043, June 2005.

[26] N. Magnus, K. P. Niels, and R. Ole, "New developments in state estimation for nonlinear systems," *Automatica*, vol. 36, no. 11, pp. 1627-1638, November 2000.

[27] R. Cheng and J. Huang, "New developments in state estimation for nonlinear systems," *Proc. of 10th International Conference on Modelling, Identification and Control*, pp. 1-6, 2018.

[28] S. Shamma and K. Y. Tu, "Approximate set-valued observers for nonlinear systems," *IEEE Transactions on Automatic Control*, vol. 42, no. 5, pp. 648-658, May 1997.

[29] S. Li, C. K. Ahn, and Z. Xiang, "Command filter based adaptive fuzzy finite-time control for switched nonlinear systems using state-dependent switching method," *IEEE Transactions on Fuzzy Systems*,vol. 29, no. 4, pp. 833-845, April 2021.

[30] S. Li, C. K. Ahn, J. Guo, and Z. Xiang, "Global output feedback sampled-data stabilization of a class of switched nonlinear systems in the p-normal form," *IEEE Transactions on Systems, Man, and Cybernetics: Systems*, vol. 51, no. 2, pp. 1075-1084, February 2021.

[31] S. Li, C. K. Ahn, and Z. Xiang, "Sampled-data adaptive output feedback fuzzy stabilization for switched nonlinear systems with asynchronous switching," *IEEE Transactions on Fuzzy Systems*, vol. 27, no. 1, pp. 200-205, January 2019.

[32] G. Nagamani, M. Shafiya, G. Soundararajan, and M. Prakash, "Robust state estimation for fractional-order delayed BAM neural networks via LMI approach," *Journal of the Franklin Institute*, vol. 357, no. 8, pp. 4964-4982, May 2020.

[33] F. Xu, J. Tan, T. Raïssi, and B. Liang, "Design of optimal interval observers using set-theoretic methods for robust state estimation," *International Journal of Robust and Nonlinear Control*, vol. 30, no. 9, pp. 3692-3705, March 2020.

[34] S. Y. Liu, Y. L. Zhang, L. Xu, F. Ding, A. Alsaedi, and T. Hayat, "Extended gradient-based iterative algorithm for bilinear state-space systems with moving average noises by using the filtering technique," *International Journal of Control, Automation, and Systems*, vol. 19, no. 4, pp. 1597-1606, 2021.

[35] J. Y. Mao, D. R. Ding, and G. L. Wei, "Distributed stubborn-set-membership filtering with a dynamic event-based scheme: The Takagi Sugeno fuzzy framework," *International Journal of Adaptive Control and Signal Processing*, vol. 35, no. 4, pp. 513-531, December 2020.

Shuai Zhang received his B.Sc. degree in automation from Jiangnan University in 2014, where he is currently pursuing an M.Sc. degree in Jiangnan University. His research interests include system modeling and state estimation.

Zi-Yun Wang received his B.Sc. degree in electronic information engineering from Jiangnan University in 2010 and his Ph.D. degree in control science and engineering from Jiangnan University in 2015. His research interests include system modeling and state estimation for practical industrial application.

Yan Wang received her Ph.D. degree in control science and engineering from Nanjing University of Science and Technology in 2006. Her research interests include system modeling and optimal scheduling.

Zhi-Cheng Ji received his Ph.D. degree in power electronics and power drives from China University of Mining and Technology in 2004. His research interests include nonlinear control, adaptive control, and system identification.